CAMBRIDGE

Cambridge University Press & Assessment
978-1-108-42336-6 — Single-Molecule Science
Edited by Krishnarao Appasani , Raghu Kiran Appasani
More Information

3 Multiscale Fluorescence Imaging

Manuel Gunkel, Jan Philipp Eberle, Ruben Bulkescher, Jürgen Reymann, Inn Chung, Ronald Simon, Guido Sauter, Vytaute Starkuviene, Karsten Rippe, and Holger Erfle

3.1 Introduction

Automated fluorescence microscopy-based screening approaches have become a standard tool in systems biology, usually applied in combination with exogenous regulation of gene expression in order to examine and determine gene function. Gain of function can be created by introducing cDNAs encoding the gene of interest that can be either untagged or tagged for the visualization of the recombinant protein and its subcellular localization (e.g., green fluorescent protein [GFP]-tagged; Temple et al., 2009). After the discovery of RNA interference (RNAi) in the late 1990s and the development of mammalian short interfering RNA (siRNA) and short hairpin RNA (shRNA) libraries in the early 2000s, gene knockdown technologies became a mainstream for loss-of-function screens on a large or genome-wide scale (Heintze et al., 2013). To date, genome-wide siRNA libraries are still the main application in genomic high-throughput screening, although key problems of the RNAi technology have become apparent, such as off-target effects, variable levels of knockdown efficiency, resulting in low-level confidence in hits of screening campaigns. In order to overcome these limitations, alternative methods for manipulation of gene expression have been developed and predominantly rely on gene excision. They are collectively called "genome editing technologies" such as zinc finger nucleases (ZFNs) or transcription activator-like effector nucleases (TALENs) (Gaj et al., 2013). However, both approaches are incompatible for the generation of large-scale libraries in a foreseeable time. A third player among gene editing technologies, clustered regularly interspaced short palindromic repeats (CRISPR) is the most promising in terms of high-throughput gene editing in human or mouse cell culture systems. In addition, CRISPR has been successfully applied to establish animal models (e.g., mouse, zebrafish, flies) and cell lines and had as well successfully been used in multiple plant species, including wheat, rice, sorghum, and tobaccos (Sander and Joung, 2014). It comprises RNA-guided Cas9 DNA nucleases originating from the microbial adaptive immune system. When bacteria are invaded by phages, they incorporate fragments of the viral genome into their

Holger Erfle, Head of the Advanced Biological Screening Facility, BioQuant, Heidelberg University, Heidelberg, Germany

© Cambridge University Press & Assessment www.cambridge.org

CAMBRIDGE
Cambridge University Press & Assessment
978-1-108-42336-6 — Single-Molecule Science
Edited by Krishnarao Appasani , Raghu Kiran Appasani
More Information

own DNA as spacers flanked by palindromic repeats. Upon a second infection, the cell transcribes these loci into CRISPR targeting RNA (crRNA), which, together with a transactivating crRNA (tracrRNA), is loaded into the Cas9 nuclease. This RNA-protein complex then binds and destroys the invading foreign DNA that matches the crRNA. Several labs discovered independently that crRNA and tracrRNA can be merged into a single guideRNA (gRNA), and that coexpression of gRNA and Cas9 suffices to effectively translate the CRISPR principle into mammalian cells for editing and excision of endogenous genes (Mali et al., 2013). As a 20 nt segment of the gRNA determines target specificity, CRISPR is easily tailored to any sequence of interest by customizing this short gRNA signature region. CRISPR has quickly established itself as an amazingly easy-to-use tool to regulate gene expression, including large-scale screening.

However, these screening approaches are often merely a starting point for further validation of the results and additional investigations. They are designed to cover a broad range of disturbances and don't allow a detailed and thus time-consuming examination of individual conditions or phenotypic occurrences.

By interlinking data acquisition and data analysis in a feedback-driven acquisition loop, the scale of these experiments has been extended toward targeted screening experiments. In this connection, a sample overview is generated followed by substructure classification and acquisition with a higher sampling rate to retrieve multiscale information of the sample. This ranges from images showing intercellular structures to subcellular resolution with additional color channels or 3D acquisition. Hence in-depth information can be extracted that would not be available from conventional fluorescence microscopy screening.

For the integration of high-resolution microscopy, techniques such as confocal microscopy or fluorescence recovery after photobleaching (FRAP) microscopy automated setups running via CellProfiler (Tischer et al., 2014) or Micropilot (Conrad et al., 2011) have been published as well as setups utilizing the integrative software platform KNIME (www.knime.org; Berthold et al., 2008) as interlink between image acquisition and analysis (Gunkel et al., 2017).

In the last decade, substantial improvements in the area of super-resolution techniques allowed to resolve targets in the 20 nm range (Rust et al., 2006). Single-molecule localization microscopy (SMLM) is one of these techniques utilizing the ability of fluorophores to switch stochastically between a fluorescing and a nonfluorescing state. Imaging these "blinking" fluorophores over time allows us to separate them from one another since it is unlikely that neighboring fluorophores are fluorescing simultaneously. To acquire enough blinking events for reconstructing a single SMLM dataset, thousands of images need to be acquired. For that reason, screening experiments applying SMLM result in time-consuming measurements for the experimenter, and selection criteria affect the duration of the screen and the quality of the data obtained.

In this chapter, an integration of fully automated targeted SMLM into a screening platform is presented in order to achieve targeted microscopy (TIM).

Holger Erfle, Head of the Advanced Biological Screening Facility,
BioQuant, Heidelberg University, Heidelberg, Germany

© Cambridge University Press & Assessment www.cambridge.org

CAMBRIDGE
Cambridge University Press & Assessment
978-1-108-42336-6 — Single-Molecule Science
Edited by Krishnarao Appasani , Raghu Kiran Appasani
More Information

As use case, the super-resolved acquisition of recognized phenotypes detected in high-throughput screening is presented, as well as fully automated high-resolution imaging on tissue microarrays (TMAs) after classification based on low-resolution images. For method details, see (Eberle et al., 2017). A focus was set on creating a modular open-source add-on that is easy to use and extendable to other imaging tasks. Therefore, plugins for KNIME were created to control a single setup that combines wide-field imaging, confocal microscopy, and SMLM.

3.2 Material and Methods

3.2.1 Cell Culture and Materials

HeLa cells (ATCC® CCL-2™) were cultivated in Dulbecco's modified Eagle's medium (Life Technologies, Carlsbad, CA) supplemented with 10 percent fetal bovine serum (Biochrom, Berlin, Germany), 2 mM L-glutamine (Life Technologies, Carlsbad, CA), and 100 U/mL, 100 μg/mL penicillin/streptinomycin. For live cell imaging, HeLa cells were used, which stably produce H2B-GFP fusion protein (Neumann et al., 2010), and their growth conditions are as mentioned before. The following siRNAs were purchased from Life Technologies, Carlsbad, CA: PLK1 siRNA Silencer® Select (# 4390826), INCENP siRNA Silencer® Select (# 4390825). The following CRISPR plasmids were purchased from Sigma-Aldrich, St.Louis, MO: pCMV-Cas9-2A-GFP-U6-PLK1-gRNA, pCMV-Cas9-2A-GFP-U6-INCENP-gRNA. Switching buffer consists of phosphate buffered saline (PBS) and 1 mol/L mercaptoethanol solution in a relation of 10:1.

3.2.2 Solid Phase Transfection in Multiwell Plates

For the transfection of cDNAs and siRNAs, respectively, 3.25 μL or 2.85 μL of OptiMEM (Invitrogen, Carlsbad, CA), containing 0.4 M sucrose and 1.50 μL or 0.40 μL of peqFECT (PEQLAB, Erlangen, Germany) were added to a single well of a 384 multiwell plate (low volume plate, Thermo Fisher Scientific, Waltham, MA). After adding 250 ng of the respective plasmids and 7.50 pmol of the respective siRNAs, the solution was incubated for 30 minutes at room temperature (RT) to allow complex formation. Then 3.625 μL of 0.2 percent gelatine (Sigma-Aldrich, St. Louis, MO), containing 1 percent fibronectin (Sigma-Aldrich, St. Louis, MO), were added into each well, and the mixture was diluted with 375 μL $_{dd}H_2O$. Of this, 40 μL was transferred to each well of 384-well plate (ibidi, Martinsried, Germany) and dried in a vacuum centrifuge (mivac quattro concentrator, Genevac, Stone Ridge, NY). 6.4×10^4 and 3.2×10^4 cells were seeded in 200 μL culture medium/per well of a 384-well plate for the experiments lasting 24 hours and 72 hours, respectively.

3.2.3 Immunocytochemistry

Cells were fixed with methanol in -20°C for 5 minutes and washed with PBS at RT. The cells were treated with 3 percent bovine serum albumin (BSA) in PBS for 60 min, then microtubules were stained with monoclonal mouse anti-α-tubulin antibody (Cell Signaling Technology, Danvers, MA) and the secondary goat

Holger Erfle, Head of the Advanced Biological Screening Facility,
BioQuant, Heidelberg University, Heidelberg, Germany
© Cambridge University Press & Assessment www.cambridge.org

CAMBRIDGE
Cambridge University Press & Assessment
978-1-108-42336-6 — Single-Molecule Science
Edited by Krishnarao Appasani , Raghu Kiran Appasani
More Information

antimouse antibody, conjugated to AlexaFluor® 647 (Life Technologies, Carlsbad, CA). For counterstaining of the nuclei, 1 μg/mL Hoechst 33342 (Life technologies, Carlsbad, CA) solution in PBS was added.

3.2.4 Sample Preparation of Tissue Microarrays

Tissue microarrays were deparaffinized by incubating them three times in xylene for 10 minutes, incubated twice in 96 percent ethanol for 5 minutes, and dried at 48°C for 3 minutes. After a proteinase K treatment that previously has been optimized for prostate cancer TMAs (1 mg/ml proteinase K in TBS for 4 hours at 37 °C), TMAs were washed twice with H2O for 3 minutes, briefly immersed in 96 percent ethanol, and air dried for a few minutes. After hydration through a grade ethanol series, slides were incubated in 1 percent Tween-20 for 1 minute before antigen masking, for which the slides were placed in 10 mM sodium citrate buffer (pH 6), boiled at 700 W in a microwave, and left at 120 W for another 9 minutes. After cooling down, incubation in increasing ethanol series and a short period of air-drying, the hybridization with the peptide nucleic acid (PNA) fluorescence in situ hybridization (FISH) probes was performed. For this, tissue sections were incubated with 0.1 μM of a Cy3-labeled telomere probe (CCCTAA)3 (TelC-Cy3, Panagene). In experiments where the centromeres were also visualized, 0.1 μM of a FAM-labeled CenpB PNA probe (ATTCGTTGGAAACGGGA) was added at the same time. The hybridization took place in 70 percent formamide, 10 mM Tris-HCl, pH 7.5, 0.1 μg/ml salmon sperm. First, slides were denatured at 84°C for 5 minutes and then left overnight at room temperature in a wet chamber for hybridization. Next, slides were washed three times for 15 minutes in PNA wash buffer, followed by three 5-minute washes in phosphate-buffered saline with Tween (PBST), and incubation with an anti-progressive multifocal leukoencephalopathy (PML) antibody (1:100, PG-M3, sc-966, Santa Cruz) in PBS overnight at 4°C in a wet chamber. Finally, the slides were washed with PBST, incubated with the secondary antibody (here: antimouse IgG coupled to Alexa647, Life Technologies) for 1 hour at RT, again washed with PBST and embedded with Prolong including DAPI.

3.2.5 Wide-Field Screening Microscopy

For the initial imaging of the samples, an Olympus IX81 ScanR system (Olympus, Hamburg, Germany) was used with a magnification of 20× (Olympus UPlan-SApo, NA 0.75). All wells of the imaging plates expected to contain phenotypic cells were imaged with an overlap between adjacent images of 10 percent resulting in 391 subpositions in order to cover the whole area of 0.55 cm^2 in 96 well plates. Two color channels for Hoechst and AlexaFluor® 647 staining were recorded at center wavelengths for detection of 405 nm and 647 nm.

3.2.6 Confocal Microscopy

For subsequent high- and super-resolution imaging, a modified Leica SP5 system Leica Microsystems, Wetzlar, Germany) was used. The microscope applies a semiconductor laser emitting at 405 nm as well as a 63× objective

Holger Erfle, Head of the Advanced Biological Screening Facility,
BioQuant, Heidelberg University, Heidelberg, Germany
© Cambridge University Press & Assessment www.cambridge.org

CAMBRIDGE
Cambridge University Press & Assessment
978-1-108-42336-6 — Single-Molecule Science
Edited by Krishnarao Appasani , Raghu Kiran Appasani
More Information

(Leica HCX PL APO 63× NA 1.47 Oil CORR TIRF). The fluorescence is filtered by an acousto-optical beam splitter and detected with photomultiplier tubes (PMTs). A live cell chamber enables imaging of living cells and protects the sample from external influences. This unit is primarily controlled by the Leica Application Suite Advanced Fluorescence (LAS AF, version 2.7.1.9530) extended with the Matrix Screener. Reference images were acquired at three positions already imaged at the wide-field system for coordinate transfer. Based on these three reference images, a coordinate transfer of all marked phenotype positions (see Section 3.3) was performed. Confocal 3D image stacks (11 layers, 1μm spacing) of the identified phenotypes were acquired. At each position, an autofocus routine was performed prior to the confocal scan. After the confocal sequence, the system was paused at each position and a subsequent localization microscopy acquisition sequence was triggered in the axial center of the confocal stack via the computer-aided microscopy (CAM) interface and the associated KNIME workflow.

For the external control of the Leica microscope, the CAM server is used. This server is included in the Matrix Screener and receives and sends messages (CAM commands) for applying so called Matrix Screener Jobs. If an image is acquired, the CAM server will send a message including its file path. Jobs and commands that were executed are communicated via this server. Confocal images are saved automatically by the Matrix Screener.

3.2.7 Single-Molecule Localization Microscopy

For *d*STORM imaging of the AlexaFluor® 647 stain, the same Leica SP5 system with an additional wide-field detection and laser illumination was used. Ports on the side of the TCS SP5 allow adding a wide-field illumination and a detection beam path. The illumination beam is generated by external lasers (Omicron LuxX with 488 nm, Cobolt Jive with 561 nm) and widened with a Galilean telescope (achromatic lenses with focal lengths of 80 mm and -20 mm). An achromatic lens with a focal length of 600 mm and a movable mirror couple the laser beam into the microscope. With different mirror positions, one can choose between normal wide-field and skewed illumination, such as highly inclined and laminated optical sheet (HILO) illumination, resulting in reduced background signals. The mirror positions are reproducible since it is moved electronically by servo motor. The emission beam path consists of an emission filter wheel (Thorlabs FW102C) and a relay lens pair (focal lengths of 150 mm) for extending the beam path. A Hamamatsu Orca Flash 4.0 scientific complementary metal-oxide-semiconductor (sCMOS) camera with a resulting pixel size of 103 nm is used for imaging. This custom-built unit is primarily controlled via the open-source microscopy software μManager (Edelstein et al., 2014), which in turn can be controlled from within a KNIME workflow. Detection could be switched between confocal and wide-field mode via the lower-right camera port of the microscope stand. For SMLM imaging, the respective well of the multiwell plate was filled with switching buffer before imaging. Image acquisition was controlled by a KNIME workflow (see also Section 3.3) and set up in such a way

Holger Erfle, Head of the Advanced Biological Screening Facility,
BioQuant, Heidelberg University, Heidelberg, Germany
© Cambridge University Press & Assessment www.cambridge.org

CAMBRIDGE
Cambridge University Press & Assessment
978-1-108-42336-6 — Single-Molecule Science
Edited by Krishnarao Appasani , Raghu Kiran Appasani
More Information

that first a confocal stack of the individual phenotypic cells was acquired, then the optical configuration was changed automatically to wide-field laser illumination and wide-field detection for SMLM image acquisition. The laser intensity was raised to 140 mW by the KNIME workflow controlling the acquisition routine, and an imaging sequence of 5,000 images with 30 ms integration time for each frame was acquired by a Hamamatsu OrcaFlash4.0 sCMOS camera. After the acquisition, laser emission was shut down and the next confocal sequence was triggered.

3.2.8 Phenotype Recognition

Data analysis workflows based on KNIME have been set up in order to identify phenotypic penetration of polo-like kinase 1 (PLK1) and inner centromere protein (INCENP) knockdown and knockout in wide-field images. In a first step, the workflow loads the image raw data files into the image processing pipeline, which performs a rolling ball background subtraction corresponding to the radius of the nuclei and then segments the nuclei and calculates various object features. In the second step, a feature space analysis is performed, which returns probability functions for the segmented objects, enabling classifying nuclei of the expected phenotype.

Binary images were generated by using three different approaches (see Figure 3.1). (i) The first is a coarse local thresholder featuring a radius of the nucleus size

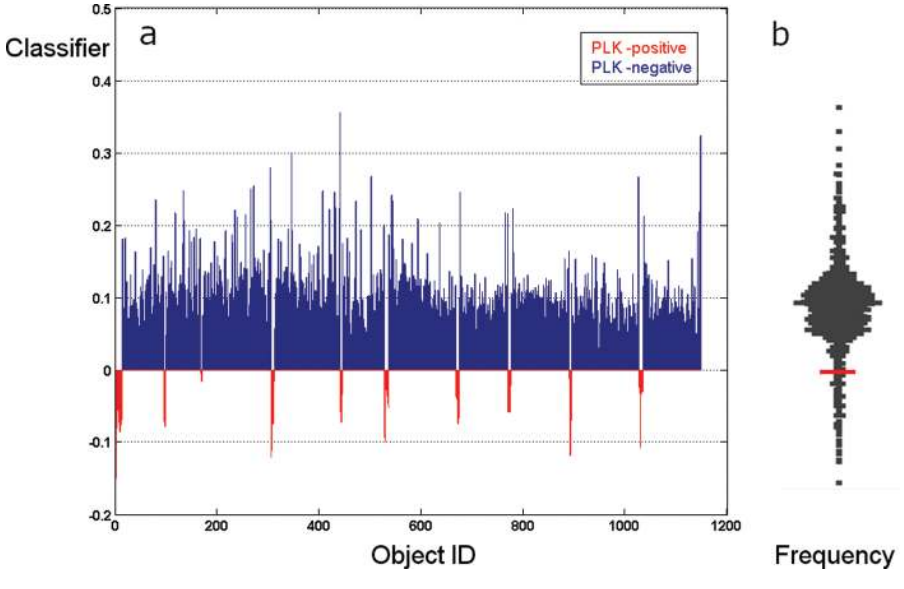

Figure 3.1 Automated hit calling after transfection of plasmid-based CRISPR. Result of the target identification: (**a**) depicts one-dimensional projections of the three-dimensional feature space of classifiers as obtained by the phenotypic classification. The dataset is normalized to the PLK1 reference feature space as represented by the classifier value 0. Each nucleus with corresponding object ID is classified as PLK1-like (red, negative values) or non-PLK1-like (blue, positive values). The resulting ratio between PLK1-like and non-PLK1-like is 6 percent phenotype positive nuclei. (**b**) depicts the corresponding frequency of nuclei with specific classifier values. "Standard" nuclei are identifiable by the wide "bulge" above the 0 line with classifier values between 0.05 and 0.15.

Holger Erfle, Head of the Advanced Biological Screening Facility,
BioQuant, Heidelberg University, Heidelberg, Germany

© Cambridge University Press & Assessment www.cambridge.org

CAMBRIDGE
Cambridge University Press & Assessment
978-1-108-42336-6 — Single-Molecule Science
Edited by Krishnarao Appasani , Raghu Kiran Appasani
More Information

provided segments matching the nucleus regions (coarse segmentation). By applying a four-connected neighborhood procedure for each pixel within each of the resulting segments, we obtained additional information about the structural homogeneity. Touching objects were separated using a watershed function, and the resulting segments were labeled by assigning a specific identifier to each of the nuclei. (ii) A fine local thresholder featuring a radius of 1/10th of the nucleus size returned segments with a size corresponding to the internal structure of PLK1 phenotypes as represented by the intensity distribution. Thus, the resulting segments displayed the rough intracellular structure (fine segmentation). (iii) In order to obtain information related to the full area an object is covering, we applied a contour search function based on the segments as obtained by the fine segmentation procedure. By mapping the labeled images of the three segmentation procedures, we assigned each intracellular compartment to the associated nucleus. Finally, texture and intensity-based features were calculated for further phenotypic classification. Positions of phenotypic cells were stored in a coordinate list.

3.2.9 Super-Resolution Reconstruction

The acquired SMLM image stacks were analyzed via the ImageJ plugin ThunderSTORM (Hagen et al., 2014). Since sCMOS cameras have pixel-dependent gain values, this is only an approximation, as ThunderSTORM uses pixel-independent values. Nonetheless, qualitative information about spatial sample relocalization is possible to gain from the analyzed data.

3.3 Results and Discussion

The Leica TCS SP5 with custom-built extensions is able to perform wide-field, confocal, and super-resolution microscopy. In order to manage screening experiments in a fully automated manner, a central control unit is required. Here the Java-based graphical programming language KNIME was chosen, which can also be used by nonprogrammers. In KNIME, a complex process is divided into tasks that are executed by specific nodes that are connected to a KNIME workflow. An active community provides nodes for image processing and machine learning algorithms. Also individual nodes can be added by writing an ImageJ2 plugin or by using the KNIME application programming interface (API).

Plugins have been programmed for controlling the confocal and SMLM unit in a KNIME workflow. Figure 3.2 shows how the units were connected to KNIME.

3.4 Tool for Controlling the SMLM Unit

Here an ImageJ2 plugin was written that utilizes the MMCore Java API of μManager. As a starting point, an existing ImageJ2 plugin for KNIME (https://github.com/knime-ip/knip-micromanager) was used. The created plugin provides three KNIME nodes for controlling the SMLM devices. A configuration node (MMConfiguration) initializes all devices, and a stop system node

Holger Erfle, Head of the Advanced Biological Screening Facility,
BioQuant, Heidelberg University, Heidelberg, Germany
© Cambridge University Press & Assessment www.cambridge.org

CAMBRIDGE
Cambridge University Press & Assessment
978-1-108-42336-6 — Single-Molecule Science
Edited by Krishnarao Appasani , Raghu Kiran Appasani
More Information

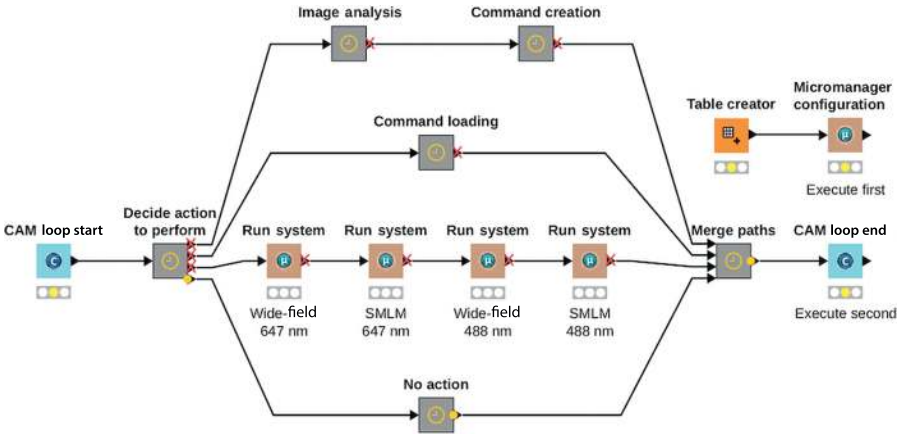

Figure 3.2 Schematic overview of the device control via KNIME. The confocal setup is controlled by the CAM server, and the SMLM device control is integrated with an ImageJ2 plugin. The measurement data are saved from for both units on an external server.

(MMStopSystem) deinitializes them after the measurement. A run node (MMRunSystem) applies all devices in a certain order and saves the acquired images. During measurement, a live image is displayed. Currently the plugin is dependent on the specific devices used in this setup, but it is possible to adapt a similar setup that runs with μManager.

3.5 Tool for Interacting with the Confocal Unit

Using the KNIME API, a loop start (CAMLoopStart) and a loop end node (CAMLoopEnd) were written for communicating with the CAM server. Both nodes connect to the CAM server for reading and writing CAM commands via a Java socket. The Internet Protocol (IP) address of the computer on which the LAS AF software runs as well as the port number of the CAM server need to be set in CAMLoopStart to built a connection. An initial CAM command is sent for starting a preset screen in the Matrix Screener, then it works as a listener. CAMLoopEnd is able to send multiline CAM commands to the CAM server and stops the server connection if the scan has finished. Since the loop nodes are iterating continuously, they are able to mesh at desired positions with the screen. Those positions can be set by applying a WaitForCAM job in the Matrix Screener for pausing the screen.

3.6 Workflow for Targeted Super-Resolution Microscopy

The presented tools enable to control the microscopic setup via KNIME. In this way, a KNIME workflow (Figure 3.2) has been designed for finding targets on confocal images and applying super-resolution microscopy on them. Prior to running the KNIME workflow, a screen needs to be set up on the Matrix Screener. Here jobs were defined for switching between the confocal detection unit and the super-resolution setup.

Holger Erfle, Head of the Advanced Biological Screening Facility,
BioQuant, Heidelberg University, Heidelberg, Germany

© Cambridge University Press & Assessment www.cambridge.org

CAMBRIDGE
Cambridge University Press & Assessment
978-1-108-42336-6 — Single-Molecule Science
Edited by Krishnarao Appasani , Raghu Kiran Appasani
More Information

Basically the KNIME workflow starts with CAMLoopStart. It initializes the screen and provides the complete file path of acquired confocal images. Image analysis and machine learning algorithms identify targets on the images, which allows relocating the target structure in the the super-resolution beam path. The corresponding CAM commands are created, and CAMLoopEnd sends them to the CAM server, where they are executed. MMRunSystem acquires subsequently super-resolution images, and the screen continues with the next position.

Hence, multicolor imaging in confocal and super-resolution mode of one target per screening position is possible with this setup. The experiment runs fully automated, and no external influence is necessary. Furthermore, it is easy to alter image analysis for the needs of biological tasks. But it is important to test whether targets are reliably focused by the Matrix Screener autofocus methods.

3.7 Application of TIM Microscopy to Potentiate Plasmid-Based CRISPR Usage for Screening

In order to examine fine structures like microtubular organization, a sufficient degree of resolution is needed, which can often not be provided by high-throughput images, since these are optimized for fast acquisition, and are thus acquired at low or medium resolution and cover a wide field of view in order to detect as many specimens simultaneously as possible. To gain more information on the microtubule structure in the experiments, we developed an automated targeted light microscopy approach (TIM) combining fast wide-field with slow confocal and single-molecule localization microscopy. This enabled us to select sparsely distributed phenotypic cells and zoom in on these individual cells with higher resolution. We applied confocal microscopy for high multicolor 3D resolution and super-resolution *d*STORM microscopy for 2D imaging of the microtubule structures.

Firstly, we identified phenotypic cells acquired with a standard wide-field Olympus IX81 ScanR screening microscope by advanced image processing in KNIME. This includes image segmentation for identification of cells and texture- and intensity-based feature extraction for phenotypic classification and hit identification. The positions of the resulting "hit" cells are registered and exchanged with high-content microscopy. In our realization of the concept, image acquisition is followed and refined by either confocal or single-molecule localization microscopy.

The sample was transferred to a Leica SP5 confocal microscope with an additional localization microscopy unit, and positions were matched by referencing the slide using the fixed cells on the sample as reference points. For each identified phenotypic cell, a multicolor 3D confocal image was recorded, and directly afterward an image sequence for *d*STORM single-molecule

Holger Erfle, Head of the Advanced Biological Screening Facility,
BioQuant, Heidelberg University, Heidelberg, Germany
© Cambridge University Press & Assessment www.cambridge.org

CAMBRIDGE
Cambridge University Press & Assessment
978-1-108-42336-6 — Single-Molecule Science
Edited by Krishnarao Appasani , Raghu Kiran Appasani
More Information

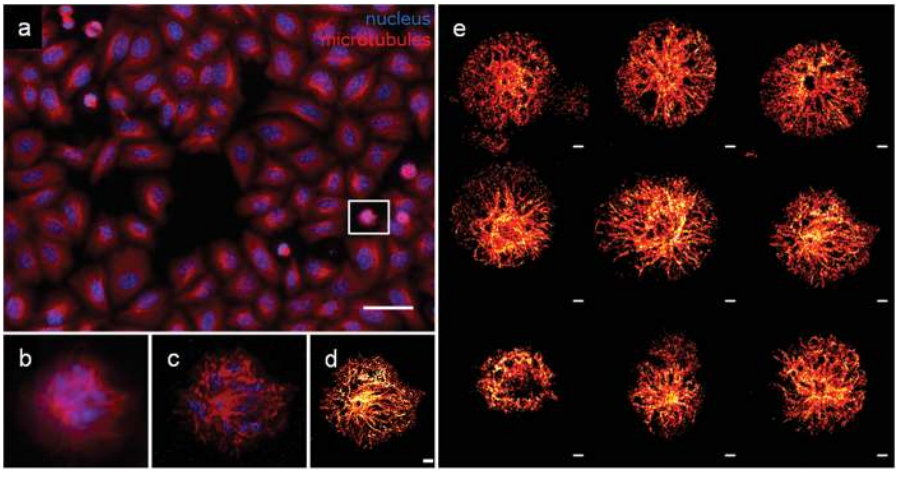

Figure 3.3 Example for CORE microscopy. (**a**) wide-field image from the prescreen (scale bar 50 µm). (**b**) Selected phenotypic cell from the widefield screen as indicated in (**a**) by the white rectangle. (**c**) The same cell acquired in confocal mode; only one layer from the confocal stack is shown here. (**d**) The same cell acquired in *d*STORM mode. (**e**) example gallery of automatically acquired cells in dSTORM mode.

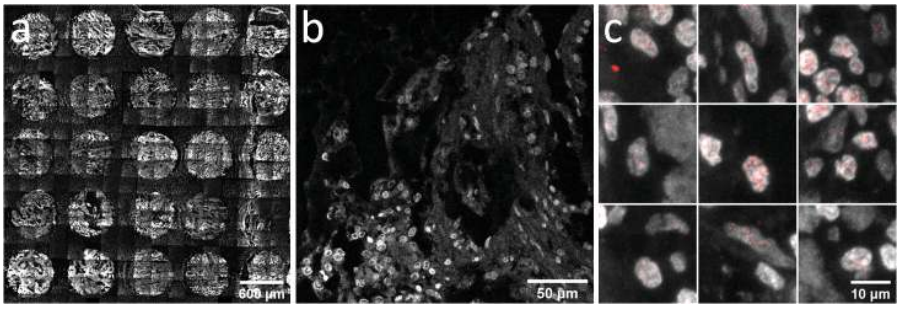

Figure 3.4 Tissue microarray. (**a**) Sub-region of 5x5 cores, imaged with 20x20 tiles. One example of these 400 tile images is shown in (**b**), with the nuclei stained by DAPI. In the individual images, cell nuclei are automatically recognized and 3D stacks of 41 planes for DAPI (nuclear stain) and CY3 (telomeres) color channels are imaged. Z-Projections of exemplary nuclei are shown in (**c**).

localization was acquired fully automatic and controlled by a KNIME workflow with direct feedback to the microscope software via the Leica CAM interface (see Figure 3.3 and 3.4).

We examined change of microtubule phenotype after treatment with CRISPR reagent against PLK1 and used as described previously as a filter for nucleus phenotype change after knockout with CRISPR. Inactivation of PLK1 by either -RNAi or pharmacologic inhibition causes a prolonged arrest of cells in

Holger Erfle, Head of the Advanced Biological Screening Facility,
BioQuant, Heidelberg University, Heidelberg, Germany

© Cambridge University Press & Assessment www.cambridge.org

CAMBRIDGE
Cambridge University Press & Assessment
978-1-108-42336-6 — Single-Molecule Science
Edited by Krishnarao Appasani , Raghu Kiran Appasani
More Information

prometaphase, which is due to activation of the spindle assembly checkpoint (Lenart et al., 2007).

Acknowledgments

This work was supported by HD-HuB (grant number 031A537C) in the de.NBI program and CancerTelSys (grant number 01ZX1302) in the e:Med program of the German Federal Ministry of Education and Research (BMBF), "Methoden für die Lebenswissenschaften," of the Baden-Württemberg Stiftung (grant number P-LS-SPII/11). The ViroQuant-CellNetworks RNAi Screening Facility was supported by the CellNetworks–Cluster of Excellence (grant number EXC81).

REFERENCES

Berthold, M. R., Cebron, N., Dill, F., et al. (2008). *KNIME: The Konstanz Information Miner.* Berlin, Heidelberg, Springer Berlin Heidelberg.

Conrad, C., Wünsche, A., Tan, T. H., et al. (2011). Micropilot: Automation of Fluorescence Microscopy-Based Imaging for Systems Biology. *Nature Methods* **8**(3), 246–249.

Eberle, J. P., Muranyi, W., Erfle, H., and Gunkel, M. (2017). Fully Automated Targeted Confocal and Single-Molecule Localization Microscopy. In H. Erfle, ed., *Super-Resolution Microscopy*. Humana Press, New York, NY**:** 139–152.

Edelstein, A. D., Tsuchida, M. A., Amodaj, N., Pinkard, H., Vale, R. D., and Stuurman, N. (2014). Advanced Methods of Microscope Control Using μManager Software. *Journal of Biological Methods* **1**(2), e10. doi: 10.14440/jbm.2014.36.

Gaj, T., Gersbach, C. A., and Barbas, C. F. III (2013). ZFN, TALEN, and CRISPR/Cas-Based Methods for Genome Engineering. *Trends Biotechnol* **31**(7), 397–405.

Gunkel, M., Chung, I., Wörz, S., et al. (2017). Quantification of Telomere Features in Tumor Tissue Sections by an Automated 3D Imaging-Based Workflow. *Methods* **114**, 60–73.

Hagen, G. M., Borkovec, J., Ovesný, M., Křížek, P., and Švindrych, Z. (2014). ThunderSTORM: A Comprehensive ImageJ Plug-in for PALM and STORM Data Analysis and Super-Resolution Imaging. *Bioinformatics* **30**(16), 2389–2390.

Heintze, J., Luft, C., and Ketteler, R. (2013). A CRISPR Case for High-Throughput Silencing. *Front Genet* **4**, 193.

Lenart, P., Petronczki, M., Steegmaier, M., et al. (2007). The Small-Molecule Inhibitor BI 2536 Reveals Novel Insights into Mitotic Roles of Polo-Like Kinase 1. *Current Biology* **17**(4), 304–315.

Mali, P., Yang, L., Esvelt, K. M., et al. (2013). RNA-Guided Human Genome Engineering via Cas9. *Science* **339**(6121), 823–826.

Neumann, B., Walter, T., Hériché, J.-K., et al. (2010). Phenotypic Profiling of the Human Genome by Time-Lapse Microscopy Reveals Cell Division Genes. *Nature* **464**(7289), 721–727.

Rust, M. J., Bates, M., and Zhuang, X. (2006). Sub-Diffraction-Limit Imaging by Stochastic Optical Reconstruction Microscopy (STORM). *Nature Methods* **3**, 793.

Sander, J. D. and Joung, J. K. (2014). CRISPR-Cas Systems for Editing, Regulating and Targeting Genomes. *Nature Biotechnology* **32**(4), 347–355.

Temple, G., Gerhard, D. S., Rasooly, R., et al. (2009). The Completion of the Mammalian Gene Collection (MGC). *Genome Research* **19**(12), 2324–2333.

Tischer, C., Hilsenstein, V., Hanson, K., and Pepperkok, R. (2014). Adaptive Fluorescence Microscopy by Online Feedback Image Analysis. In J. C. Waters and T. Wittman, eds., *Methods in Cell Biology*. Academic Press. Vol. **123**, 489–503.

Holger Erfle, Head of the Advanced Biological Screening Facility,
BioQuant, Heidelberg University, Heidelberg, Germany

© Cambridge University Press & Assessment www.cambridge.org